Published in final edited form as:
Nat Med. 2008 October ; 14(10): 1118–1122. doi:10.1038/nm.1864.

Bortezomib-induced enzyme-targeted radiotherapy in herpesvirus-associated tumors

De-Xue Fu[1], **Yvette Tanhehco**[1,5], **Jianmeng Chen**[1], **Catherine A. Foss**[2], **James J. Fox**[2], **Ja-Mun Chong**[1,6], **Robert F. Hobbs**[2], **Masashi Fukayama**[3], **George Sgouros**[2], **Jeanne Kowalski**[1], **Martin G. Pomper**[1,2], and **Richard F. Ambinder**[1]

[1]Johns Hopkins School of Medicine, Department of Oncology, Baltimore, MD, 21231, USA

[2]Johns Hopkins School of Medicine, Department of Radiology, Baltimore, MD, 21231, USA

[3]Department of Human Pathology, Graduate School of Medicine, University of Tokyo, Japan

Abstract

We investigated the possibility of using a pharmacologic agent to modulate viral gene expression in order to target radiotherapy to tumor tissue. In a murine xenograft model, we had previously shown targeting of [^{125}I]2'-fluoro-2'-deoxy-beta-D-5-iodouracilarabinofuranoside ([^{125}I]FIAU) to tumors engineered to express the Epstein-Barr virus (EBV)-thymidine kinase (TK). Here we extend those results to targeting of a therapeutic radiopharmaceutical [^{131}I]FIAU to slow or stop tumor growth or to achieve tumor regression. These outcomes were achieved in xenografts with tumors that constitutively expressed the EBV-TK, as well as with naturally-infected EBV tumor cell lines. Burkitt's lymphoma and gastric carcinoma required activation of viral gene expression by pretreatment with bortezomib. Marked changes in tumor growth could also be achieved in naturally-infected Kaposi's sarcoma herpesvirus (KSHV) tumors following bortezomib activation. Bortezomib-induced enzyme-targeted radiation (BETR) therapy illustrates the possibility of pharmacologically modulating tumor gene expression to effect targeted radiotherapy.

Introduction

Targeting of radiopharmaceuticals provides an important tool for the therapy of malignancy. Targeting tissue-specific surface antigens such as CD20 on B cells with radioimmunoconjugates has expanded the application of therapeutic radiation[1,2]. However, radioimmunoconjugates may be limited by the target level of expression, antibody affinity, or the physical characteristics of the antibody (that may impede delivery to large tumors or protected compartments) [3]. Targeting metabolic pathways such as those involved in

Correspondence should be addressed to: R.F.A., 389 Bunting Blaustein Cancer Research Building, 1650 Orleans, Baltimore, MD 21287, E-mail: ambinri@jhmi.edu.

Author Contributions D.F. designed and performed murine imaging and therapy experiments, Y.T. designed and performed murine imaging experiments, J.C. assisted with the design and interpretation of murine experiments, J.F. synthesized radiotracers and carried out imaging and image analysis, C.F.synthesized radiotracers and assisted with imaging and image analysis, J-M. C. designed and performed murine experiments involving gastric carcinoma xenografts, R.F. Hobbs carried out dosimetry analysis, M.F. made the transplantable gastric carcinoma xenografts available and assisted in the design of experiments, G.S. assisted in the design and interpretation of experiments and the writing of the manuscript, J.K. provided statistical guidance, M. P. assisted in the design and interpretation of experiments and editing of the manuscript, R.A. designed and conceptualized the approach, analyzed and interpreted data and wrote the manuscript. The final version of the manuscript was seen and approved by all authors.

[5]Present addresses: University of Pittsburgh, School of Medicine
[6]Department of Pathology, Tokyo Metropolitan Toshima Hospital, Japan.

COMPETING INTERESTS STATEMENT The authors declare no competing financial interests.

concentrating iodine in thyroid tissue is an alternative approach the more general application of which has been limited by the ability to identify appropriate tumor-specific pathways.

Epstein-Barr virus (EBV) is associated with various lymphomas and carcinomas. Kaposi's sarcoma herpesvirus (KSHV, HHV-8) is associated with sarcoma and lymphoma. The viral genome serves as a nearly tumor-specific target[4]. Thus virus-associated metabolic pathways approximate tumor-specific metabolic pathways. The ability to target radioisotopes to herpesvirus pathways has been demonstrated using vectors engineered with the herpes simplex 1 (HSV1) thymidine kinase (TK) gene to monitor gene expression in the gene therapy setting[5,6]. Direct application to virus-associated tumors has been limited by the virtual absence of expression of the TK in tumor cells.

We previously demonstrated that naturally occurring tumor cells harboring EBV could be imaged with a radiolabeled nucleoside analogue, if a pharmacologic inducer of the viral TK was utilized[7]. In the present investigation, we extend that observation to demonstrate that an inducing agent with a radiotherapeutic nucleoside analogue allows targeted therapy of virus harboring tumor cells in xenograft models.

RESULTS

Engineered constitutive EBV TK expression

To evaluate specificity with regard to the concentration of 2'-fluoro-2'-deoxy-beta-D-5-iodouracil-arabinofuranoside (FIAU) in tumor tissue, we used a human osteosarcoma cell line engineered to express the EBV-TK[8]. Tumor cells were engrafted on the flanks of SCID mice. After tumor was palpable, [^{125}I]FIAU was administered intravenously and mice were sacrificed (Fig.1). Selective concentration of radioactivity in tumor was apparent by 2 hours and radioactivity levels in the tumor remained constant until the last time point at 96 hours, whereas levels in nontarget tissues decrease. In a parallel experiment carried out to later times, radioactivity in tumor was stable from 2 hours to the last time point at 4 days (not shown). The tumor to muscle ratio climbed from 4.6 at 2 h p.i. to peak at 205 at 24 h p.i. and fall to 114 at 96 h p.i. consistent with previous investigators' reports in a similar murine model with tumor constitutively expressing the HSV1-TK[6].

To determine whether concentration of radioisotope in tumor tissue was adequate to achieve a therapeutic effect, mice were treated with [^{131}I]FIAU or buffered saline (Fig. 2a). Control and TK tumors in mice injected with buffered saline, and control tumors in mice injected with [^{131}I]FIAU showed similar growth curves, and of note, the 95% confidence intervals of the slopes of those growth curves (as determined by linear regression) overlapped. However, the growth slope of TK tumors in mice injected with [^{131}I]FIAU flattened (i.e. the confidence interval for the slope of TK with [^{131}I]FIAU in particular includes a zero slope estimate and does not overlap with the confidence intervals of the other growth curves). In separate experiments, increasing doses of [^{131}I]FIAU were associated with increasing effects on tumor growth (Fig. 2b). When chimeric tumors were generated from admixtures of TK and control tumor cells, increasing percentages of TK-expressing tumor cells in the admixture were also associated with increasing effects on tumor growth (Fig. 2c).

Bortezomib-induced enzyme targeted radiotherapy for EBV-Burkitt's lymphoma

Can a therapeutic effect be achieved in a naturally infected tumor? In previous studies we identified bortezomib as a potent inducer of lytic EBV infection[7]. In order to evaluate the specificity in naturally infected tumor tissue, EBV (+) Burkitt's lymphoma cells were engrafted SC on the flanks of SCID mice. After tumor was palpable, [^{125}I]FIAU was administered intravenously 24 hr after bortezomib and mice were sacrificed. Selective concentration of

radioactivity was apparent in these tumors (Table 1). Therefore, we proceeded with an evaluation of a therapeutic isotope. As above, mice with Burkitt's lymphoma xenografts received either buffer or bortezomib followed the next day by treatment with [^{131}I]FIAU or no treatment. As can be seen in Fig. 3a, tumor growth curves in mice injected with buffer followed by [^{131}I]FIAU were similar to tumor growth curves in mice injected with buffer alone. Bortezomib without [^{131}I]FIAU slowed tumor growth. Bortezomib followed by [^{131}I]FIAU stopped tumor growth (the 95% confidence interval overlapped 0 but did not overlap the 95% confidence intervals of the slopes of the growth curves associated with buffer alone or buffer with [^{131}I]FIAU). In experiments with a second EBV(+) Burkitt's lymphoma cell line (Akata), parallel results were achieved (data not shown). Thus, bortezomib allowed targeting of [^{131}I]FIAU with therapeutic effect.

Bortezomib-induced enzyme targeted radiotherapy for EBV gastric carcinoma

Although EBV is associated with Burkitt's', AIDS-related, Hodgkin's lymphoma, NK and other lymphomas, the numerically most important associations are with nasopharyngeal cancer (~80,000 new cases/year) and approximately 10% of gastric carcinoma (~93,000 new cases/year)[9-11]. In order to determine whether the bortezomib-induction strategy might also be applicable to epithelial malignancies, we studied a transplantable human EBV-associated gastric cancer (KT) xenograft[12]. Following engraftment, mice were induced with bortezomib followed by [^{125}I]FIAU and tumors were imaged with single photon emission computed tomography (SPECT) (Fig.4a). Tissue distribution studies showed selective concentration of [^{125}I]FIAU in tumor, although the ratios in tumor to other tissues were not as dramatic as with the Burkitt's lines (Table 1). When induction was followed by [^{131}I]FIAU, tumor growth slowed (Fig.3b).

Bortezomib-induced enzyme targeted radiotherapy in KSHV malignancy

Could the approach be extended to KSHV-associated tumors? We studied two primary effusion lymphoma (PEL) cell lines that harbor KSHV. In a SCID xenograft model, bortezomib allowed imaging of both BCBL1 and BC3 with [^{125}I]FIAU (Fig.4b). Tissue distribution studies showed selective concentration in tumor tissue (Table 1), and when induction was followed by treatment with [^{131}I]FIAU tumors growth slowed (Fig.3c).

Discussion

The HSV1-TK has been used as a tool in gene therapy[13]. Even the notion that a viral TK might be used to target radiation therapy has been explored by others [14]. Similarly, induction of the EBV-TK with a histone deacetylase inhibitor followed by treatment with ganciclovir has been reported to induce remissions in some patients[15]. Here, we model a new approach: bortezomib-induced enzyme targeting of radionuclide (BETR) therapy. We show that this BETR approach yields promising results in lymphoid and epithelial malignancies in murine xenografts of human tumors.

How do the doses administered in the murine model extrapolate to the clinical setting? Experience with 131I-labeled antibodies against lymphoma in patients demonstrates that clinical responses are achievable with 0.5 to 2 Gy to the tumor[16]. The biodistribution data presented in Fig. 1 allow estimates of the absorbed dose to tumor and vital organs, and suggests that the kidneys and red marrow are the dose limiting organs for [^{131}I]FIAU. As detailed in the online supplement, it should be possible to deliver 0.5 to 2 Gy to a 1 gram tumor in a 70 kg patient with critical organ doses well below toxicity.

FIAU was previously investigated as an antiviral[17]. Chronic dosing of FIAU was associated with hepatic damage and in some cases fatality[18-20]. In those trials, treatment for less than

four weeks with a cumulative dose less than 200 mg was not associated with either clinical or biochemical evidence of toxicity. Thus, the “no-effect dose” of FIAU might be conservatively estimated to be on the order of 0.1 mg/kg per administration. [^{124}I]FIAU has been administered to patients for imaging without any adverse effect on hepatic function[21]. Extrapolating from our xenograft experiments, a radiotherapeutic effect is likely to be achieved at doses of FIAU that are orders of magnitude times less than the no-effect FIAU dose in humans.

BETR treatment results in concentration of FIAU in lymphoma and carcinoma xenograft models and impacts on tumor growth curves for each of the tumors studied (Fig. 3). However, in the lymphoma models, growth stops, whereas in the gastric carcinoma model growth only appears to be slowed. This difference likely reflects two phenomena. First, epithelial tumors are more resistant to radiation than lymphoid tumors. Second, the percentage of injected radioactivity per gram of tumor achieved in the lymphomas is greater than in the carcinoma (Table 1, Fig. 4). Optimization for human tumors will ultimately require further xenograft and clinical studies, but the ability to image EBV-TK activation directly in patients and thus assess the relevant pharmacokinetics of radiolabeled FIAU offers the promise that optimization can be rapid.

One concern with all 131I-labeled radiopharmaceuticals is deiodination. In the case of tositumomab, dehalogenases decouple the radioisotope from the antibody moiety, resulting in free, circulating 131I. In order to block this accumulation, standard procedure involves pretreatment of patients with thyroid protective agents (potassium iodide) beginning before drug administration and continuing until 2 weeks after administration. In comparison, biotransformation of FIAU is limited because of the high chemical and metabolic stability of the *N*-glycosyl linkage in pyrimidine nucleosides that contain the 2'-fluoro substituent in the arabinosyl (“up”) configuration[22]. Studies in serum and whole blood over a 24 h period indicate excellent stability and low susceptibility to deiodination. FIAU is also cleared more rapidly from the plasma than tositumomab (3.9 versus 48 hours). Thus with less deiodination and more rapid clearance, it may be expected to have a better safety profile with respect to radiation exposure in normal tissues than agents already in the clinic.

BETR therapy also offers possible advantages over other lytic induction-suicide prodrug approaches. All lytic induction approaches are limited by the tendency of gammaherpesviruses to latency. When ganciclovir or a similar agent mediates cell killing, a therapeutic effect will likely require that a large fraction of tumor cells express viral enzymes. Although the phenomenon of bystander killing attributed to the exchange of phosphorylated nucleotides and nucleotide analogues between cells via gap junctions has been recognized[23], such killing is limited. In the gene therapy setting attempts have been made to engineer increased expression of the connexin protein in the gene therapy vector so as to increase such killing[24]. However, this approach to increasing bystander killing is not readily applicable in approaches that do not involve gene therapy. Indeed, some of the therapeutic agents used to treat tumors may interfere with such bystander killing[25]. [^{131}I]FIAU bystander killing is not limited by connexin expression or gap junctions but is a function of beta emissions with a maximum energy of 0.61 MeV that deposit 90% of their energy in a sphere of radius 0.7 mm[26]. This “cross-fire” effect is likely an important contributor to the efficacy of radioimmunotherapy in lymphoma[27]. “Cross-fire” with [^{131}I]FIAU may be inferred from Fig. 2c where the tumor growth rate is substantially slowed when even 10% of tumor cells harbor the EBV-TK. Cell level dosimetry modeling is presented in the online supplementary material.

A second limitation of the lytic induction-suicide prodrug approaches is that ganciclovir-mediated killing is cell cycle dependent. As reported by several groups of investigators, activation of lytic infection in EBV and KSHV infected cells leads to cell cycle arrest[28-30],

thus likely compromising cell cycle-dependent tumor kill. In contrast, radiation effects are not similarly diminished by lytic induction.

BETR therapy may also offer advantages over radioimmunotherapeutic approaches. Internalization of radioimmunoconjugates may lead to degradation and release of free isotope with consequent loss of specificity. In contrast, we observed that following injection of FIAU, isotope is stably associated with EBV-TK expressing tumor (Fig.1a). Enzymatic phosphorylation and incorporation into DNA (as has been reported in HSV1-TK expressing cells [6]) offers the possibility of achieving high concentrations in tumor tissue not limited by concentration gradients. Finally, both FIAU and bortezomib are small molecules and thus better tumor penetration would be anticipated in comparison with antibody conjugates. FIAU does not penetrate the blood-brain barrier but does reach brain tumors reflecting disruption of the blood brain barrier[22]. More broadly, the use of small molecules to activate tissue or tumor-specific metabolic pathways suggests the possibility that metabolic targeting of radiation may have applications beyond thyroid cancer.

Methods

Cell lines and plasmids

Lymphoma cell lines were maintained in suspension culture in RPMI 1640 (Life Technologies, Gaithersburg, MD) with 10% fetal bovine serum, 100 units/mL penicillin, 100 Ag/mL streptomycin, and 100 mmol/L L-glutamine as previously described[7]. TK-143B and V143B cells are stably transfected lines derived from the human osteosarcoma (143B) cell line carrying either a plasmid expressing EBV-TK or a control vector (PCDNA3), as previously described[8]. These were maintained in DMEM (Life Technologies) supplemented with 10% fetal bovine serum (Gemini BioProducts, Calabasas, CA), 100 units/mL penicillin, 100 Ag/mL streptomycin, 2 mmol/L L-glutamine, and 400 Ag/mL G418 for selection. The KT transplantable EBV(+) gastric adenocarcinoma was passaged in SCID mice[12].

Chemicals

Bortezomib was administered IV at 1.67 μg/gram. FIAU, and 2'-fluoro-2'-deoxyuracil-β-D-arabinofuranoside were obtained from Moravek Biochemicals (Brea, CA). [^{125}I] and [^{131}I]NaI were purchased from MP Biomedicals (Costa Mesa, CA). [^{125}I]FIAU and [^{131}I]FIAU was synthesized as previously described[7]. For imaging or treatment, FIAU was administered 24 hours after bortezomib. In each of the experiments described bortezomib was administered as a single dose.

Tumor generation

Cultured cell lines were tested for mycoplasma and found to be negative. Cells (5×10^6) were resuspended in 200 μL Matrigel matrix (BD Biosciences, Bedford, MA) and injected SC in 6- to 7-week-old male severe combined immunodeficient mice. Caliper measurements of the longest perpendicular tumor diameters were performed every other day. Tumor volume was estimated according to the formula for a three dimensional ellipse: $4\pi/3 \times (\text{width}/2)^2 \times (\text{length}/2)$. Treatment and imaging studies were performed when tumors reached a size of ~1 cm in diameter.

Ex vivo biodistribution

As previously described[7], [^{125}I]FIAU in PBS was injected into the tail vein, 3 to 4 mice were sacrificed at each indicated time point, organs were removed and weighed, and tissue radioactivity measured using an automated gamma counter. The percent injected dose per gram

(%ID/g) of tissue was calculated by comparison with samples of a standard dilution of the initial dose.

Planar gamma imaging, SPECT-computed tomography and image analysis

As previously described[7], imaging was done as an adjunct to the ex vivo biodistribution studies. The X-SPECT (Gamma Medica Instruments, Northridge, CA) has a γ-ray detector head dimension of 20.5 × 15 × 9 cm and a field of view of 120 × 125 mm. The high-resolution parallel hole collimator used has the following specifications: 1.22mm hole diameter, 0.20mm septa thickness, 25.4mm bore hole length. The detector material composed of NaI[Tl] has a pixel size of 2 × 2 × 6 mm. Mice were placed in a prone position on the parallel hole collimator and kept under anesthesia with isoflurane. Ten-minute high-resolution scans of each mouse were obtained. SPECT-CT was done using the above-mentioned γ-ray detector and the CT detector sequentially without removing the mouse from the gantry. Analysis of imaging data was with ImageJ v1.30 (NIH, Bethesda, MD) or AMIDE (A Medical Image Data Examiner) for SPECT-CT (free software provided by SourceForge).

Biostatistics

Linear regression and curve fitting were undertaken carried using GraphPad Prism software version 5.00 for Windows, GraphPad Software, San Diego California USA, www.graphpad.com.

Supplementary Material

Refer to Web version on PubMed Central for supplementary material.

Acknowledgments

We thank Richard Wahl, S. Diane Hayward, Wen-Son Hsieh and Meir Shamay for suggestions, Susanne Bonekamp, Keng Fai Kwok and Jianhua Yu for reconstruction of imaging data, Sen Wang for assistance in the syntheses of [^{125}I]FIAU and [^{131}I]FIAU, Gilbert Green for assistance with murine imaging and therapy, and Sridhar Nimmagadda for assistance with mice experiments. This work was supported by grants from the US National Institutes of Health (NIH/NCI P50 CA96888, P01 CA113239 and U24 CA92871).

References

1. Witzig TE, et al. Long-term responses in patients with recurring or refractory B-cell non-Hodgkin lymphoma treated with yttrium 90 ibritumomab tiuxetan. Cancer 2007;109:1804–1810. [PubMed: 17380530]
2. Kaminski MS, et al. 131I-tositumomab therapy as initial treatment for follicular lymphoma. N Engl J Med 2005;352:441–449. [PubMed: 15689582]
3. Juweid M, et al. Micropharmacology of monoclonal antibodies in solid tumors: direct experimental evidence for a binding site barrier. Cancer Res 1992;52:5144–5153. [PubMed: 1327501]
4. Feng WH, Hong G, Delecluse HJ, Kenney SC. Lytic induction therapy for Epstein-Barr virus-positive B-cell lymphomas. J Virol 2004;78:1893–1902. [PubMed: 14747554]
5. Tjuvajev JG, et al. Imaging the expression of transfected genes in vivo. Cancer Res 1995;55:6126–6132. [PubMed: 8521403]
6. Haubner R, Avril N, Hantzopoulos PA, Gansbacher B, Schwaiger M. In vivo imaging of herpes simplex virus type 1 thymidine kinase gene expression: early kinetics of radiolabelled FIAU. Eur J Nucl Med 2000;27:283–291. [PubMed: 10774880]
7. Fu DX, et al. Virus-associated tumor imaging by induction of viral gene expression. Clin Cancer Res 2007;13:1453–1458. [PubMed: 17332288]
8. Moore SM, Cannon JS, Tanhehco YC, Hamzeh FM, Ambinder RF. Induction of Epstein-Barr virus kinases to sensitize tumor cells to nucleoside analogues. Antimicrob Agents Chemother 2001;45:2082–2091. [PubMed: 11408227]

9. Ushiku T, et al. p73 gene promoter methylation in Epstein-Barr virus-associated gastric carcinoma. Int J Cancer 2007;120:60–66. [PubMed: 17058198]
10. Parkin DM, Bray F, Ferlay J, Pisani P. Global cancer statistics, 2002. CA Cancer J Clin 2005;55:74–108. [PubMed: 15761078]
11. Takada K. Epstein-Barr virus and gastric carcinoma. Mol Pathol 2000;53:255–261. [PubMed: 11091849]
12. Chong JM, et al. Interleukin-1beta expression in human gastric carcinoma with Epstein-Barr virus infection. J Virol 2002;76:6825–6831. [PubMed: 12050395]
13. Blasberg RG, Tjuvajev JG. Herpes simplex virus thymidine kinase as a marker/reporter gene for PET imaging of gene therapy. Q J Nucl Med 1999;43:163–169. [PubMed: 10429512]
14. Schipper ML, Goris ML, Gambhir SS. Evaluation of herpes simplex virus 1 thymidine kinase-mediated trapping of (131)I FIAU and prodrug activation of ganciclovir as a synergistic cancer radio/chemotherapy. Mol Imaging Biol 2007;9:110–116. [PubMed: 17294333]
15. Perrine SP, et al. A phase 1/2 trial of arginine butyrate and ganciclovir in patients with Epstein-Barr virus-associated lymphoid malignancies. Blood 2007;109:2571–2578. [PubMed: 17119113]
16. Sgouros G, et al. Patient-specific, 3-dimensional dosimetry in non-Hodgkin's lymphoma patients treated with 131I-anti-B1 antibody: assessment of tumor dose-response. J Nucl Med 2003;44:260–268. [PubMed: 12571219]
17. McKenzie R, et al. Hepatic failure and lactic acidosis due to fialuridine (FIAU), an investigational nucleoside analogue for chronic hepatitis B. N Engl J Med 1995;333:1099–1105. [PubMed: 7565947]
18. Cui L, Yoon S, Schinazi RF, Sommadossi JP. Cellular and molecular events leading to mitochondrial toxicity of 1-(2-deoxy-2-fluoro-1-beta-D-arabinofuranosyl)-5-iodouracil in human liver cells. J Clin Invest 1995;95:555–563. [PubMed: 7860738]
19. Johnson AA, et al. Toxicity of antiviral nucleoside analogs and the human mitochondrial DNA polymerase. J Biol Chem 2001;276:40847–40857. [PubMed: 11526116]
20. Lewis W, et al. Fialuridine and its metabolites inhibit DNA polymerase gamma at sites of multiple adjacent analog incorporation, decrease mtDNA abundance, and cause mitochondrial structural defects in cultured hepatoblasts. Proc Natl Acad Sci U S A 1996;93:3592–3597. [PubMed: 8622980]
21. Diaz LA, et al. Imaging of Musculoskeletal Bacterial Infections by [I]FIAU-PET/CT. PLoS ONE 2007;2:e1007. [PubMed: 17925855]
22. Jacobs A, et al. Quantitative kinetics of [124I]FIAU in cat and man. J Nucl Med 2001;42:467–475. [PubMed: 11337525]
23. Westphal EM, Blackstock W, Feng W, Israel B, Kenney SC. Activation of lytic Epstein-Barr virus (EBV) infection by radiation and sodium butyrate in vitro and in vivo: a potential method for treating EBV-positive malignancies. Cancer Res 2000;60:5781–5788. [PubMed: 11059774]
24. Gentry BG, Im M, Boucher PD, Ruch RJ, Shewach DS. GCV phosphates are transferred between HeLa cells despite lack of bystander cytotoxicity. Gene Ther 2005;12:1033–1041. [PubMed: 15789060]
25. Robe PA, et al. Dexamethasone inhibits the HSV-tk/ganciclovir bystander effect in malignant glioma cells. BMC Cancer 2005;5:32. [PubMed: 15804364]
26. Dixon KL. The radiation biology of radioimmunotherapy. Nucl Med Commun 2003;24:951–957. [PubMed: 12960593]
27. Song H, et al. Therapeutic potential of 90Y- and 131I-labeled anti-CD20 monoclonal antibody in treating non-Hodgkin's lymphoma with pulmonary involvement: a Monte Carlo-based dosimetric analysis. J Nucl Med 2007;48:150–157. [PubMed: 17204712]
28. Rodriguez A, Jung EJ, Flemington EK. Cell cycle analysis of Epstein-Barr virus-infected cells following treatment with lytic cycle-inducing agents. J Virol 2001;75:4482–4489. [PubMed: 11312318]
29. Wu FY, et al. CCAAT/enhancer binding protein alpha interacts with ZTA and mediates ZTA-induced p21(CIP-1) accumulation and G(1) cell cycle arrest during the Epstein-Barr virus lytic cycle. J Virol 2003;77:1481–1500. [PubMed: 12502863]
30. Wang SE, Wu FY, Yu Y, Hayward GS. CCAAT/enhancer-binding protein-alpha is induced during the early stages of Kaposi's sarcoma-associated herpesvirus (KSHV) lytic cycle reactivation and

together with the KSHV replication and transcription activator (RTA) cooperatively stimulates the viral RTA, MTA, and PAN promoters. J Virol 2003;77:9590–9612. [PubMed: 12915572]

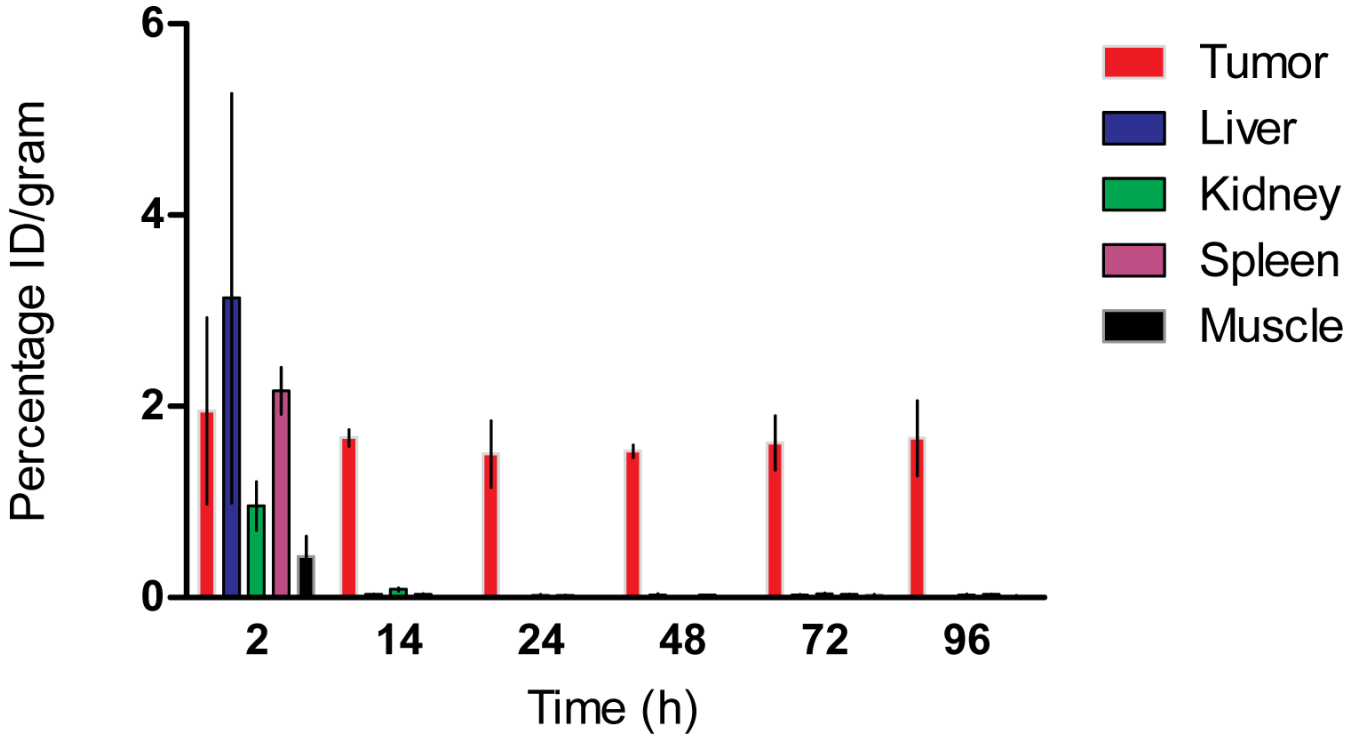

Figure 1.
[^{125}I]FIAU tissue distribution in a murine xenograft model. [^{125}I]FIAU (5μCi) was administered intravenously to SCID mice engrafted with EBV-TK(+) tumors. Animals (3-4 at each time point) were sacrificed and tissue distribution measured. The percent of the injected dose (ID) per gram tissue is shown.

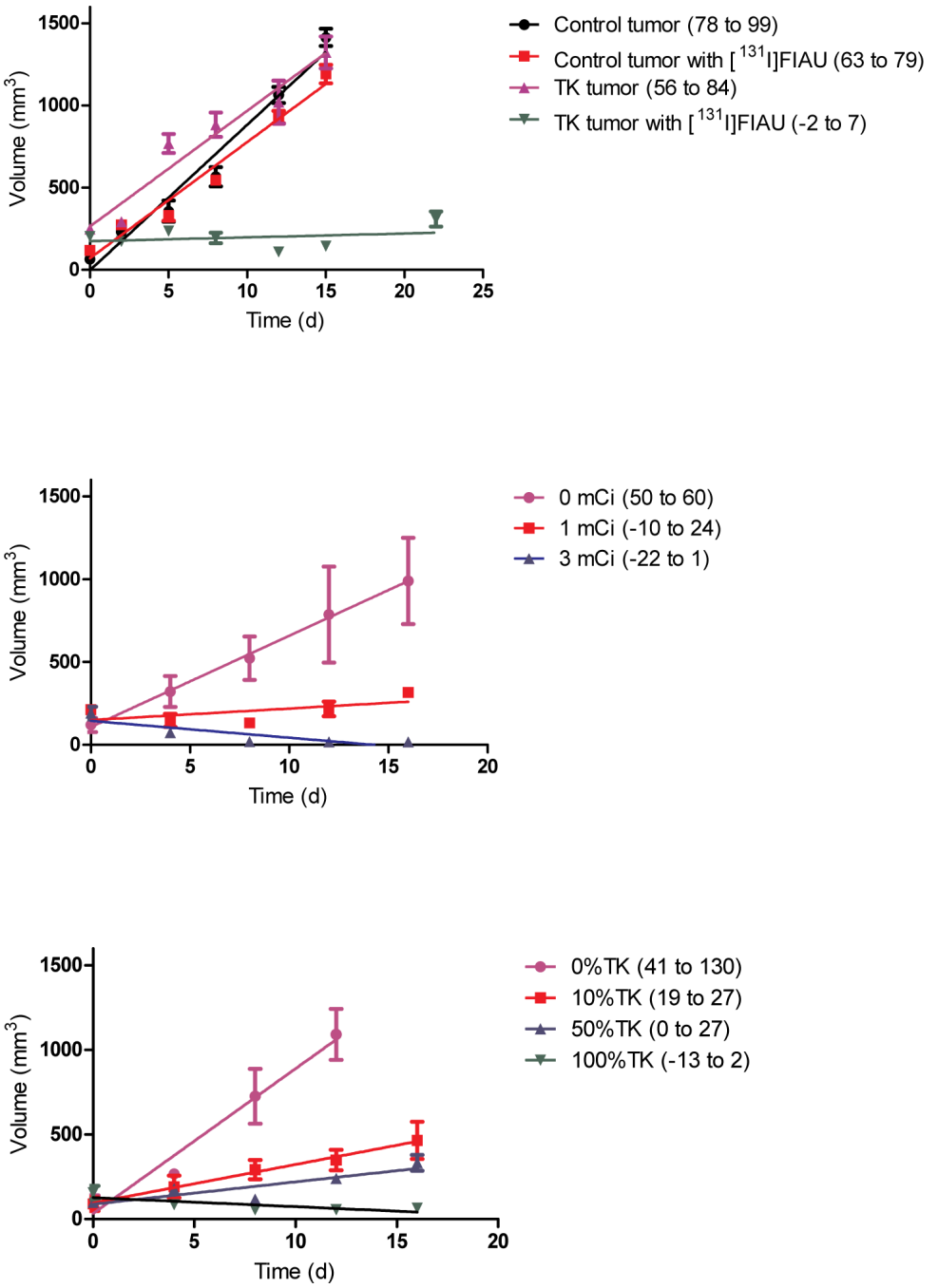

Figure 2.

Tumor growth curves. (a) Mice with control tumors (human osteosarcoma 143B cells with empty vector) or TK expressing tumors (human osteosarcoma 143B cells expressing EBV TK) were treated IV with 1.6 mCi [^{131}I]FIAU or buffered saline. (b) Dose response. Mice with EBV-TK expressing tumors were treated with buffered saline, 1 mCi [^{131}I]FIAU or 3 mCi [^{131}I]FIAU. (c) Mice with tumors resulting from engraftment of admixtures of EBV-TK expressing and control tumor cells were treated with 1.7 mCi [^{131}I]FIAU. Each time point corresponds to 3 animals. The mean, SEM, and least squares linear regression are plotted. The confidence intervals (CI, 95%) of the slopes of best fit linear regression of tumor growth curves are shown in parentheses in the legend.

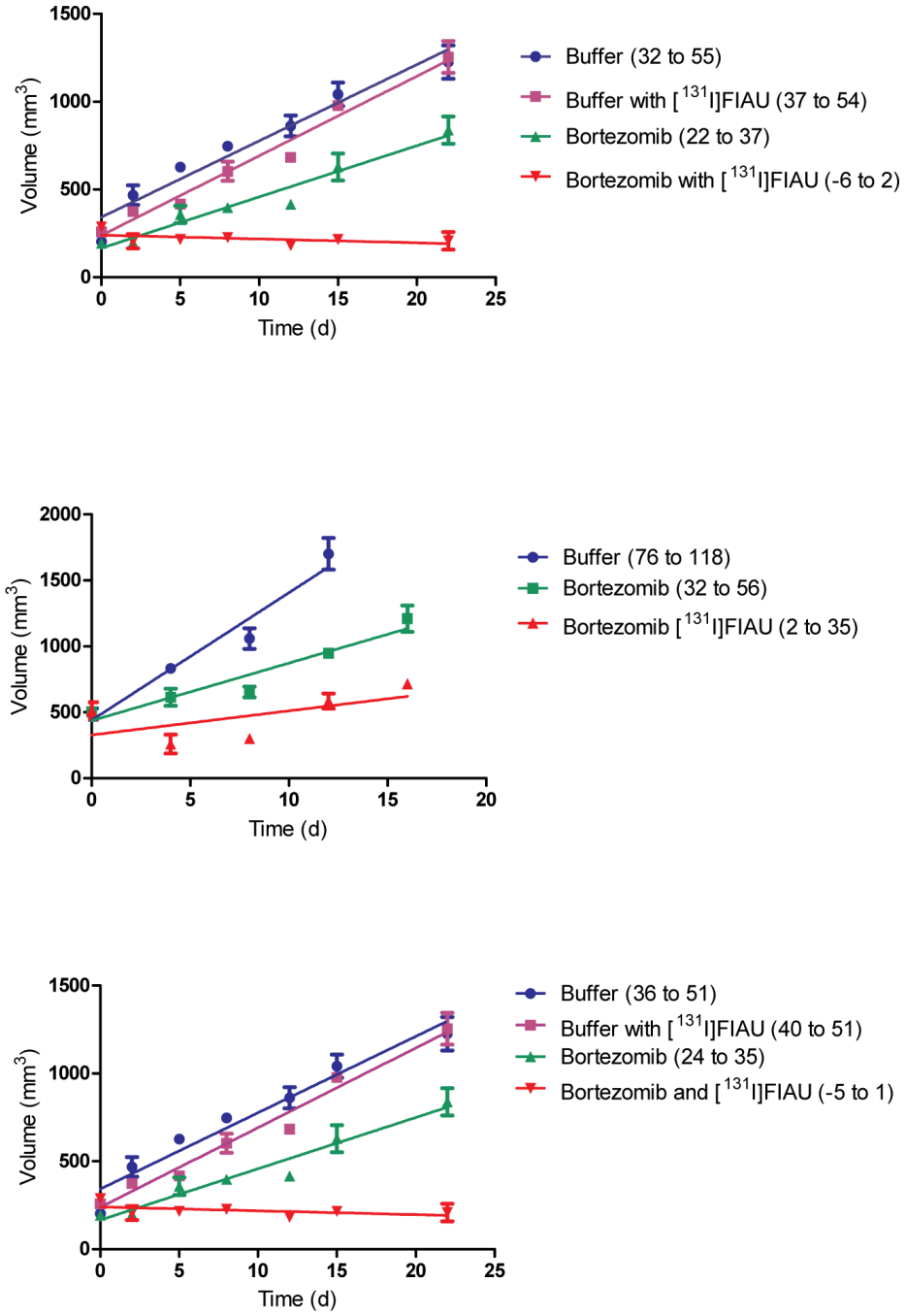

Figure 3.

Tumor growth curves in murine xenografts. (a) EBV(+) Burkitt's lymphoma (Rael), (b) EBV (+) gastric adenocarcinoma (KT), and (c) KSHV(+) primary effusion lymphoma (BCBL1) were injected intravenously with buffered saline, buffered saline followed 24 hours later by [^{131}I]FIAU, bortezomib, or bortezomib followed 24 hours later by [^{131}I]FIAU. Each time point corresponds to 3 animals. Mice were treated with 1.6 mCi (a,c) or 1.7 mCi (b). The mean, SEM, and least squares linear regression are plotted. The confidence intervals (CI, 95%) of the slopes of best fit linear regression of tumor growth curves are shown in parentheses in the legend.

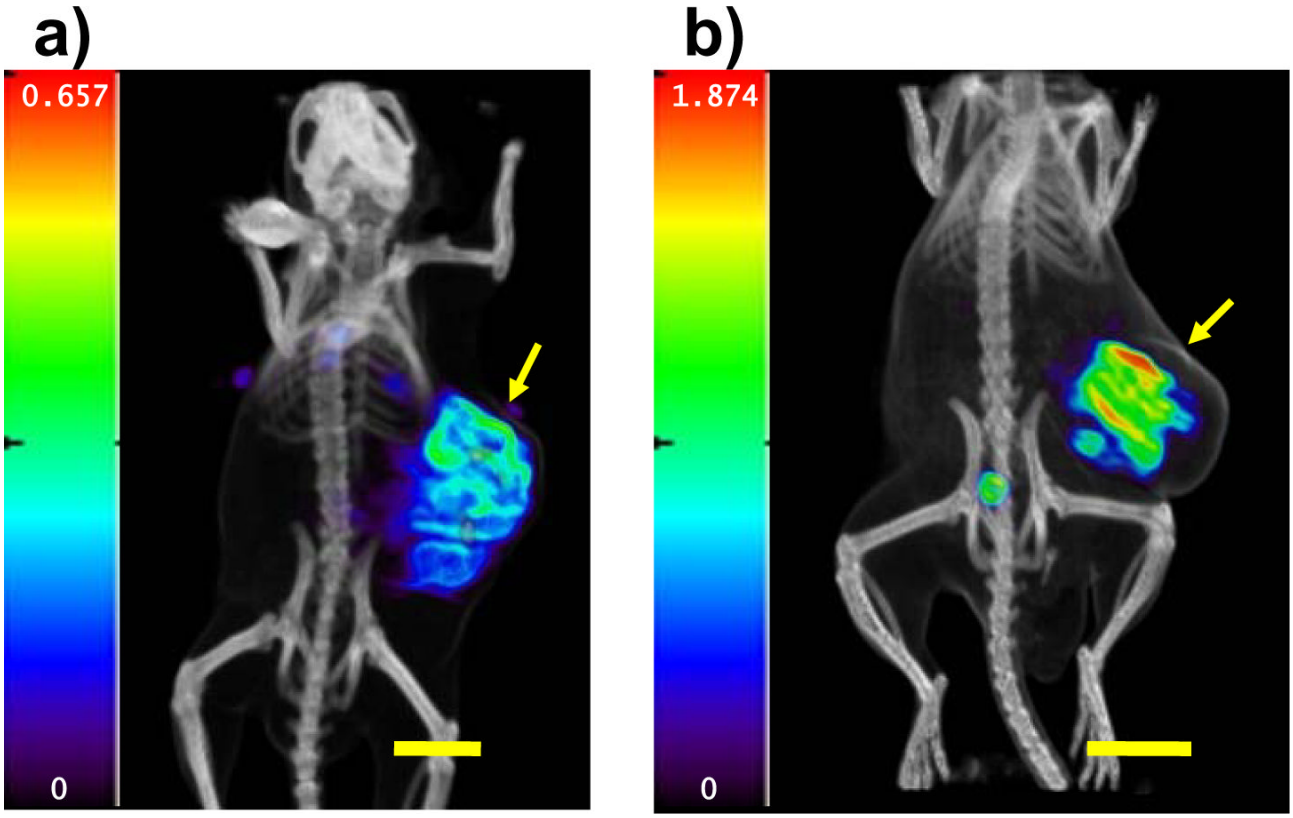

Figure 4.
[^{125}I]FIAU SPECT-CT imaging of tumors following bortezomib treatment. (a) EBV(+) gastric carcinoma (KT) tumor at 72 h p.i. (b) KSHV(+) lymphoma (BCBL1) at 48 h p.i.. Yellow arrows indicate tumor location. Color bars indicate the range of [^{125}I]FIAU uptake as % ID/g (0.68% in (a) and 1.53% in (b)). The horizontal bars indicates 1 cm.

Table 1

Tissue distribution of [^{125}I]FIAU (5μCi) in mice bearing human tumors post injection (p.i.)

Tumor	**TK143b Osteosarcoma**	**Rael Burkitt's lymphoma**	**KT gastric cancer**	**BC3 lymphoma**	**BCBL1 lymphoma**
Days p.i.	4	4	4	5	4
N	3	4	3	3	5
Virus	**EBV TK**	**EBV**		**KSHV**	
TK expression	**<-constitutive->**	**<----------bortezomib induction----------->**			
Tissue	**%ID/g±SD**				
Tumor	1.667±0.681	1.200±0.356	0.598±0.472	1.213±0.214	1.100±0.361
Liver	0.013±0.006	0.052±.027	0.050±0.017	0.009±0.002	0.0617±0.022
Spleen	0.027±0.015	0.064±.011	0.080±0.035	0.008±0.002	0.064±0.014
Kidney	0.033±0.058	0.146±.054	0.090±0.030	0.027±0.003	0.167±0.038
Muscle	0.015±0.014	0.084±.012	0.080±0.062	0.008±0.004	0.078±0.005

Nat Med. Author manuscript; available in PMC 2009 July 14.